Journal of Atomic, Molecular, Condensed Matter & Nano Physics
Vol. 9, No. 1, pp. 41–50, 2022
ISSN 2582-8215
Published by RGN Publications

http://www.rgnpublications.com

Special Issue:

Nuclear Track Detectors, Luminescence and Their Applications
Guest Editors: P.D. Sahare, Rajesh Kumar, Ashok Kumar

DOI: 10.26713/jamcnp.v9i1.1958

Research Article

Linearly Modulated OSL in $K_3Na(SO_4)_2:Eu^{3+}$ Phosphor Irradiated With 48 MeV Li^{3+} and 85 MeV C^{6+} Swift Heavy Ions Beam

Martina Saran*[1,2] and P.D. Sahare[2]

[1] *Inter-University Accelerator Centre, Aruna Asaf Ali Marg, Delhi 110067, India*
[2] *Department of Physics and Astrophysics, University of Delhi, Delhi 110007, India*
***Corresponding author:** martinasaran@gmail.com

Received: October 1, 2021 **Accepted:** May 14, 2022

Communicated by: Tarun Kumar

Abstract. $K_3Na(SO_4)_2:Eu^{3+}$ shows OSL when irradiated with swift heavy ion beams of Li^{3+} and C^{6+} at different fluences. The micro sample is prepared through solid state diffusion method along with its counter parts of ball milled (7 days) nanophosphor and co-precipitated nanophosphor samples. The material was characterized by XRD to confirm its formation in a single phase. Comparison of the experimental data with that of the data available in the literature (JCPDS data file #74 0398) shows formation of a single hexagonal phase, with the space group P3 m1. Study on the particle size effect shows that particle size in the 75–106 μm rangeis more suitable for the linearly modulated-optically stimulated luminescence (LM-OSL) dosimetry in micro form. Dosimetric properties of the phosphor material using LM-OSL technique for blue light stimulation ($\lambda = 470$ nm and $t = 120$ seconds) show that it is highly sensitive in the linear dose range. Here in this paper, we tried to find a relationship between detrapping probabilities and photoionization cross section using curve fitting (deconvolution) method. We also calculated and converted the fluence into doses using SRIM software. Data are presented indicating that the LM-OSL peak is composed of three overlapping components originating from populated traps with optical cross sections of 10^{-17}–10^{-18} cm^2. It was found that micro and ball milled nanophosphor Carbon ion beam irradiated samples dominates the photoionization cross section as compared with lithium ion irradiated samples, but co-precipitated sample is dominant in lithium irradiated samples. Which infers about the different trapping level formation and also recombination processes involved during the preparation and in readouts of samples.

Keywords. LM-OSL, Photoionization cross-section, Detrapping probabilities, Li^{3+} and C^{6+}, SHI

PACS. 87.53.Bn (Dosimerty/exposure assessment), 78.60.Lc (Optically stimulated luminescence)

1. Introduction

Optically Stimulated Luminescence (OSL) is the light emission from an irradiated material upon illumination with light of suitable wavelength(s). The phenomenon has been known for a long time and has been suggested for radiation detection, first in the mid-twentieth century. OSL Linear modulation OSL (LM-OSL) was proposed by Bulurin 1996 which consists of ramp shaping the stimulation intensity linearly while monitoring the OSL intensity. The obtained shape of the LM-OSL curves increases linearly with the stimulation intensity goes to a peak and decreases at further illumination, due to depletion in the traps (dosimetric). In continuous wave (CW) OSL, the luminescence is recorded very prompt and looks like a decay curve. Also in CWOSL, the background count rate or net background is nearly constant. In the case of LMOSL, the recording of luminescence is slow but peak shaped and the background count rate increases (non-linearly) with stimulation time. Well separated multiple peaks can also be obtained if optically sensitive traps having different values of photo ionization cross-sections are also present in the OSL process. The peak height of the LMOSL curve is decided by the number density of the traps participating in OSL process and the recombination efficiency whereas the peak position is decided by the optical stimulation rate, retrapping and recombination cross-sections and the radiation dose. It is worth mentioning that due to long recording time the LMOSL is not useful in dosimetric applications however it is very useful in characterization of traps participating in OSL process [5].

A new technique for measuring the OSL, which is based on the linear increase of the stimulation light intensity from zero to a maximum value during readout namely the linear modulation technique (LMT), has been introduced by Bulur [1]. Unlike the decay curves obtained with conventional OSL, the LMT gives peak-shaped luminescence curves. The parameters of the new luminescence curve, i.e. the peak height $L_{\max}$ and the peak position $t_{\max}$, are related to the physical parameters of the trap responsible for luminescence production, i.e. the number of trapped electrons and the detrapping rate of the electrons from the traps [1]. The analysis of LM-OSL data usually assumes a linear relationship between the detrapping rate and the stimulation light intensity [2].

The application of OSL in luminescence dating and retrospective dosimetry led to the development of readers capable of automatically carrying out OSL measurements on large numbers of samples and helped in promoting the technique. OSLDs have also been investigated for swift heavy charged particle (SHCP) dosimetry in space and charged particle therapy, both are challenging problems [10].

2. Experimental

The micro crystalline $K_3Na(SO_4)_2$:Eu material was prepared through solid state diffusion method as it has been reported that the material prepared by melt and slow cooling, method does not form a congruent single phase of $K_3Na(SO_4)_2$:Eu but a mixture of $K_3Na(SO_4)_2$, $KNaSO_4$ and a solid solution of these two systems. Therefore, to prepare the material, firstly, $EuCl_3$ was dissolved with Na_2SO_4 in 100 ml double distilled water and the solvent (water) was

evaporated at ~100 ^{0}C for doping. Resulting compound with appropriate amount of K_2SO_4 was then mixed thoroughly in a Teflon lined container using a ball milling machine and zircon balls. The mixture was then heated in a quartz crucible at around ~900 ^{0}C for several hours. The phosphor $K_3Na(SO_4)_2$:Eu (0.1%) having different particle sizes was obtained by crushing and sieving (45-150 μm) and ball milling (for different time intervals) which was later annealed at 400 ^{0}C for 2 h and quenched to room temperature (RT). The material was ball milled using zircon balls for several days (approx. for a week's time) till it was found that the particles are crushed to nanosize which was confirmed from the broadening of the XRD peaks and also by FESEM images which shown in our earlier published paper on TL [7]. The material thus prepared in different particle size ranges was used for further studies after giving proper heat treatment. The material ($K_3Na(SO_4)_2$:Eu) in nanocrystalline powder form was also prepared through solution co-precipitation method for comparison using the following chemical equation:

$$3K_2SO_4 + Na_2SO_4 \xrightarrow{\text{EtOH}} 2K_3Na(SO_4)_2 \downarrow .$$

The material samples prepared by solid state diffusion followed by crushing and sieving manually/ball milling are designated as BM samples whereas those by co-precipitation method by CP samples.

Pellets of approximately ~12.0 mm thickness and ~0.2 mm diameter were prepared taking 30 mg of the sample and 0.3 mg of Teflon powder, mixing together, putting in a die, and applying 2 ton/cm^2 pressures each time by a hydraulic press. The pellets were again annealed at 400 C for 1 hour and quenched rapidly to anneal out the deformations, if any, due to applied stress.

3. Results and Discussion

3.1 XRD Analysis

Figure 1 show the XRD patterns of the $K_3Na(SO_4)_2$:Eu micro, ball milled for 7 days and the material prepared through the co-precipitation method, respectively. The stick pattern plotted using the data in the literature (JCPDS file # 74-0398) is also given in the figure for ready reference [6]. It could be seen from the figure that most of the peaks for different (hkl) planes found in our data exactly match with those in the JCPDS file. Broadenings of the XRD peaks in the experimental data was also used to determine the sizes of the nanoparticles using the Scherrer's formula: $D = 0.9\lambda/\beta\cos(\theta)$; where D is the average grain size of the crystallites, λ is the incident wavelength, θ is the Bragg angle and β is the diffracted full width at half maximum (in radian) caused by the crystallites. The average size of these nanoparticles is estimated to be approximately ~30 and ~25 nm for the ball milled (BM) and the co-precipitated (CP) samples, respectively, which is very close to that observed in the FESEM images. The XRD patterns of the nanomaterials show a hexagonal structure for the crystallites. As mentioned earlier, Dhoble et al. [4] found that their $K_3Na(SO_4)_2$:Eu material prepared by melt method was not in a single phase and consisted of the mixture of $K_3Na(SO_4)_2$, $NaKSO_4$ and their solid solutions. Therefore, the microcrystalline material was prepared by solid state diffusion method and found to be in a desired single phase.

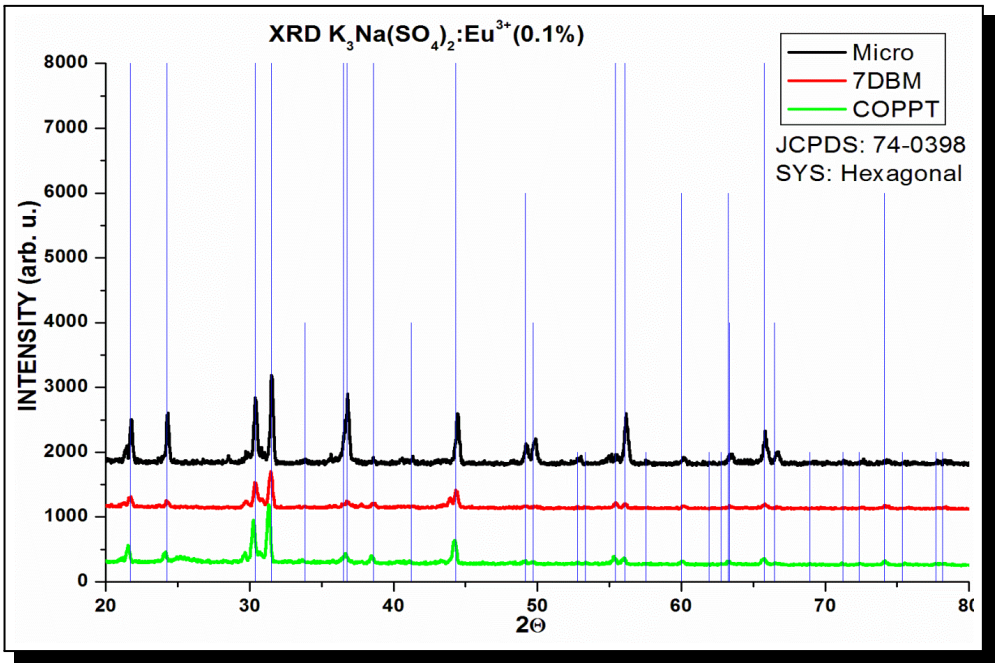

Figure 1. XRD pattern for micro, 7 day ball milled and co-precipitate sample without irradiation

The change of fluence into the dose is given in Table 1 by the formula shown. The dose to fluence value is different for lithium and carbon beam ion beams. This is converted by calculating Electronic Stopping Potential, using the stopping and range of ions in matter (SRIM) software. We also found that the ion beam could not penetrated out of the pellets as range calculated shows values lower than the thickness of pellet sample. So, it suggested that the ions got implanted in the phosphor itself.

$$D = 1.602 \times 10^{-10} \times \frac{1}{\rho}\left(\frac{dE}{dx}\right) \times n\,.$$

Table 1. Calculation for absorbed doses by the sample when exposed to different fluence (48 MeV Li^{3+} and 85 MeV C^{6+}) ion beams

Sample	Fluence (n)	DOSE (D in Gy)	Energy (Mev)
$K_3Na(SO_4)_2:Eu^{3+}$ Lithium (Li^{3+})	1×10^{10}	70	48
	1×10^{11}	70×10^{1}	48
	1×10^{12}	70×10^{2}	48
	1×10^{13}	70×10^{3}	48
$K_3Na(SO_4)_2:Eu^{3+}$ Carbon(C^{6+})	1×10^{10}	266	85
	1×10^{11}	266×10^{1}	85
	1×10^{12}	266×10^{2}	85
	1×10^{13}	266×10^{3}	85

3.2 LM-OSL DOSE Response

Discoverer Bulur suggested an innovative method of measuring optically stimulated luminescence which is now widely known as LM-OSL. The LM-OSL signal is observed by linearly increasing the stimulation power of the light source during measurement, and it has many advantages over continuous wave OSL (CW-OSL) measured with constant stimulation power. We used NUCLEONIX TL/OSL 1008 reader for obtaining the decay curves. By ramping the stimulation power from zero to a particular value (usually the maximum power of the light source), the OSL signal appears as a series of peaks; each peak represents a component of the OSL signal with a particular physical parameter, namely the photoionization cross-section. The LM-OSL signal allows more effective and accurate characterization of each OSL component than the CW-OSL signal, and thus, LM-OSL can be used as an essential tool for understanding processes giving rise to OSL and improvement of the optical dating procedure based on measurement of CW-OSL. These OSL signals arise from radiative recombination of charge carriers, de-trapped from all optically sensitive traps shown in Figure 2. Deconvolution of OSL signal is necessary to get information of individual traps plot and analyzed in Figure 3.

Deconvolution

The blue LED LM-OSL curve shapes analyzed and resolved into their individual components are presented in figures below for the maximum fluence irradiated sample $K_3Na(SO_4)_2:Eu^{3+}$ in micro, ball mill and co-precipitate forms. As observed from the figures the LM-OSL measurement does not involve any peak like structure, indeed a broad curve is obtained. For each component the time of peak maximum (t_{max}) was established. Using this parameter the detrapping probability (b) can be calculated from the expression:

$$t_{max} = \sqrt{\frac{T}{b}},$$

where T is total illumination time, which is ~120 s here. Method of calculation of photoionization cross section (s) was described by Twardak et al. [8]. Photoionization cross section is related to detrapping probability and maximum stimulation photon flux (J):

$$b = J\sigma.$$

For a monochromatic stimulation light, detrapping probability (b) is proportional to the photoionization cross-section (σ) and the light intensity (I) on the sample. Such a measurement scheme has proven to be useful in distinguishing individual OSL components in samples exhibiting more than one OSL signal with different photoionization cross-sections.

For stimulation wavelength 470 nm and power density 30 mW cm^{-2} used in the experiment the calculated photon flux was $7.1 \times 10^{16} s^{-1}\, cm^{-2}$. Using above parameters, the photoionization cross sections for all components were established given in Table 2.

Photoionization Cross-section (σ)

The photoionization cross-section is a parameter in OSL phenomenon is of major interest. For the OSL to occur, it is first necessary for an optical absorption to happen that stimulates charge carriers out of a trap, or optically ionizes them. The probability of photo ionization (P), of any given trap is simply the product of the incident light intensity and the probability that the trap will ionize by stimulation with a photon of this light. This is described by the following equation:

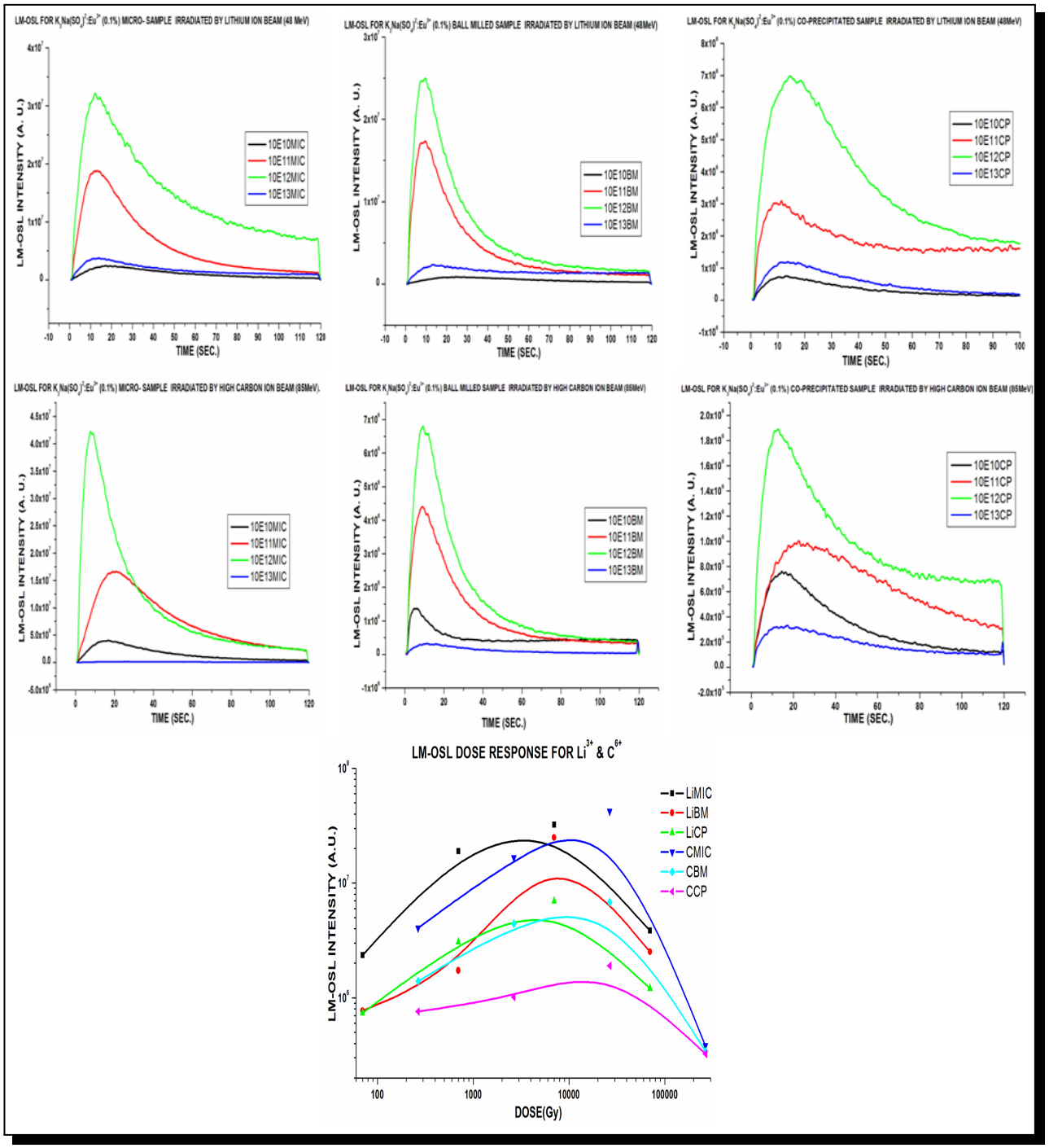

Figure 2. Dose response for micro, ball milledand co-precipitatednanophosphors at different fluencies along with its log-log graphical presentation for lithium and carbon ion beam

$$\sigma(E) = \frac{P \text{ (probability optical ionization)}}{\varphi \text{ (number of particles per unit area)}}$$

φ is the optical stimulation intensity and $\sigma(E)$ is the photoionization cross-section for interaction of the trap with an incident photon. E is the energy of the individual photons of incident light. Since the photoionization cross-section for a trap is a function of the photon energy of the incident

light, the probability of trap ionization depends on the photon energy. A material produces OSL, the optical ionization (P) will be proportional to the OSL output and is therefore an important parameter to understand. The energy (E) of one photon is given by

$$E = h\nu$$

where h is Planck's constant, 6.63×10^{-34} J s $= 6.63 \times 10^{-34}$ W s^2, and υ is frequency, it can be written as $\upsilon = c/\lambda$, where c is the speed of light and λ is wavelength. For light with wavelength (λ) 470 nm, $\upsilon = (3 \times 10^8/470 \times 10^{-9})$ s. The power of the LED used in this experiment was 30 mWcm^{-2}. Thus, the energy of one photon produced by a blue-LED ($\lambda = 470$ nm) is calculated to be 4.2×10^{-19} W s. The number of photons per unit time per unit area is 7.14×10^{16} s^{-1} cm^{-2} (0.03 W cm^{-2}/4.2×10^{-19} W s) [3].

Deconvolution of the LM-OSL curve reveals that the trapping centres are distributed over a range of photoionization cross sections [9].

Photoionization cross section for all deconvoluted peaks shows the maximum value in carbon (C^{6+} 85 MeV) irradiation case but co-precipitated sample 2 and 3 deconvoluted peak shows lower σ in case of carbon than lithium(Li^{3+} 48 MeV) ion beam irradiated sample.

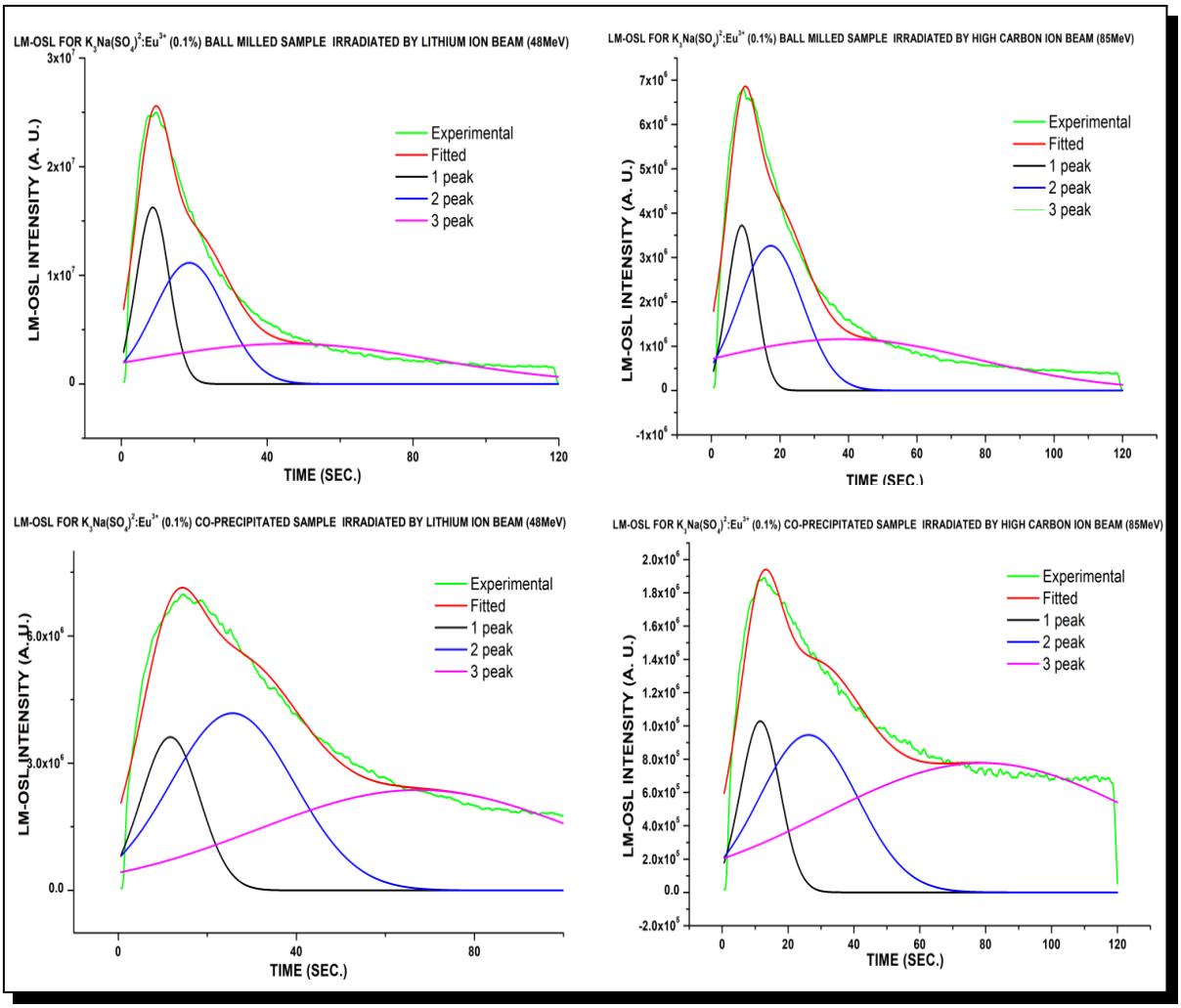

Figure 3. LM-OSL signal from $K_3Na(SO_4)_2$:Eu sample showing the components by curve fitting

Table 2. Calculated photoionization cross section in LM-OSL

Materials $K_3Na(SO_4)_2:Eu^{3+}$	Ion beam	Components (t_{max})	Detrapping probability b (s^{-1})	Photo ionization cross section (cm^2)	Relative σ
Micro	Lithium	11.56	0.9476	1.3346×10^{-17}	1
		27.09	0.4043	5.6953×10^{-18}	0.426
		70.49	0.1554	2.1887×10^{-18}	0.163
Ball mill	Lithium	8.65	1.2664	1.7836×10^{-17}	1
		18.89	0.5799	8.167×10^{-18}	0.4578
		53.44	0.2049	2.887×10^{-18}	0.1618
Co-precipitate	Lithium	11.74	0.93308	1.3142×10^{-17}	1
		25.84	0.4239	5.9708×10^{-18}	0.4543
		68.52	0.1598	2.2517×10^{-18}	0.1713
Micro	Carbon	7.53	1.4536	2.0473×10^{-17}	1
		16.25	0.6737	9.4887×10^{-18}	0.4634
		43.42	0.2522	3.5521×10^{-18}	0.1735
Ball mill	Carbon	8.46	1.2948	1.8237×10^{-17}	1
		17.34	0.6317	8.8971×10^{-18}	0.4878
		47.36	0.2312	3.2563×10^{-18}	0.1785
Co-precipitate	Carbon	11.39	0.9616	1.3543×10^{-17}	1
		26.39	0.4150	5.8450×10^{-18}	0.4315
		80.10	0.1367	1.9253×10^{-18}	0.1421

4. Conclusion

Linear modulation provides an important new approach in the analysis of OSL signals, particularly for the study of the characteristics of the minor components in a stimulation curve. A dependence of photoionization cross section (σ) on wavelength was calculated for all the irradiated samples for the fast and medium components. It was found that micro and ball milled nanophosphor Carbon ion beam irradiated samples dominates the photoionization cross-section as compared with lithium ion irradiated samples, but co-precipitated sample is dominant in lithium irradiated samples. Which infers about the different trapping level formation and also recombination processes involved during the preparation and in readouts of samples. The largest photo cross section ionization found among all was in carbon ion beam irradiated ball milled sample which 48 times ($8.8971 \times 10^{-18} - 1.8237 \times 10^{-17}$) higher as compared with all in the sample. Deconvolutions of the LM-OSL peaks revealed that they are composed of three overlapping signals from trapping states with optical cross sections in the range of 10^{-18}–

10^{-17} cm^2. The component corresponding to the largest optical cross section was about 48 times larger than that of the smallest optical cross section in all the samples.

Acknowledgements

We are thankful to the University of Delhi for partial financial assistance through R&D grants (Project # RC/2015/9677). The financial assistance by the Inter–University Accelerator Center (IUAC), New Delhi under UFUP project (File # UFR-56318) is also gratefully acknowledged. One of the author (MS) is thankful to the IUAC for a research fellowship and University of Delhi for a research fellowship.

Competing Interests

The authors declare that they have no competing interests.

Authors' Contributions

All the authors contributed significantly in writing this article. The authors read and approved the final manuscript.

References

[1] E. Bulur, A simple transformation for converting CW-OSL curves to LM-OSL curves, *Radiation Measurements* **32** (2000), 141 – 145, DOI: 10.1016/S1350-4487(99)00247-4.

[2] E. Bulur, L. Bøtter-Jensen and A.S. Murray, LM-OSL signals from some insulators: An analysis of the dependency of the detrapping probability on stimulation light intensity, *Radiation Measurements* **33** (2001), 715 – 719, DOI: 10.1016/S1350-4487(01)00089-0.

[3] D.J. Daniel, A. Raja, U. Madhusoodanan, O. Annalakshmi and P. Ramasamy, OSL studies of alkali fluoroperovskite single crystals for radiation dosimetry, *Optical Materials* **58** (2016), 497 – 503, DOI: 10.1016/j.optmat.2016.06.019.

[4] S.J. Dhoble, S.V. Moharil and T.K. Gundu Rao, Correlated ESR, PL and TL studies on $K_3Na(SO_4)_2$: Eu thermoluminescence dosimetry phosphor, *Journal of Luminescence* **93** (2001), 43 – 49, DOI: 10.1016/s0022-2313(01)00176-4.

[5] M. Kumar, B. Dhabekar, S.N. Menon, M.P. Chougaonkar and Y.S. Mayya, LiMgPO4:Tb,B OSL phosphor - CW and LM OSL studies, *Nuclear Instruments and Methods in Physics Research Section B: Beam Interactions with Materials and Atoms* **269** (2011), 1849 – 1854, DOI: 10.1016/j.nimb.2011.05.010.

[6] P.D. Sahare and M. Saran, Effect of pH on lyoluminescence of $K_3Na(SO_4)_2:Eu^{3+}$ phosphor for its application in dosimetry of high-energy radiations, *Journal of Luminescence* **179** (2016), 254 – 259, DOI: 10.1016/j.jlumin.2016.06.040.

[7] P.D. Sahare and M. Saran, Particle size effects on the dosimetry characteristics of $K_3Na(SO_4)_2$:Eu TLD micro- and nanophosphors, *Journal of Luminescence* **198** (2018), DOI: 10.1016/j.jlumin.2018.02.063.

[8] A. Twardak, P. Bilski, Y. Zorenko, V. Gorbenko and O. Sidletskiy, OSL dosimetric properties of cerium doped lutetium orthosilicates, *Radiation Measurements* **71** (2014), 139 – 142, DOI: 10.1016/j.radmeas.2014.02.018.

[9] V.H. Whitley and S.W.S. Mckeever, Linear modulation optically stimulated luminescence and thermoluminescence techniques in Al_2O_3:C, *Radiation Protection Dosimetry* **100** (2002), 61 – 66, DOI: 10.1093/oxfordjournals.rpd.a005936.

[10] E.G. Yukihara and S.W. McKeever, Optically stimulated luminescence (OSL) dosimetry in medicine, *Physics in Medicine & Biology* **53** (2008), DOI: 10.1088/0031-9155/53/20/R01.